Journal of Alloys and Compounds 509 (2011) 7645–7651

Contents lists available at ScienceDirect

Journal of Alloys and Compounds

journal homepage: www.elsevier.com/locate/jallcom

Effect of impurities content from minerals on phase transformation, densification and crystallization of α-cordierite glass-ceramic

Johar Banjuraizah[a,b], Hasmaliza Mohamad[b], Zainal Arifin Ahmad[b,*]

[a] School of Materials Engineering, Universiti Malaysia Perlis, 02600 Kangar, Perlis, Malaysia
[b] School of Materials and Mineral Resources Engineering, Universiti Sains Malaysia, Engineering Campus, 14300 Nibong Tebal, Penang, Malaysia

ARTICLE INFO

Article history:
Received 13 January 2011
Received in revised form 22 April 2011
Accepted 26 April 2011
Available online 6 May 2011

Keywords:
α-Cordierite glass-ceramic
Densification and crystallization
Impurities

ABSTRACT

α-Cordierite glass-ceramic was produced through crystallization of glass compacts made of milled glass frits. A comparative investigation between two different initial raw materials to synthesize α-cordierite glass-ceramic using the same non-stoichiometric cordierite composition fabrication process was conducted. The existence of impurities in minerals significantly affected phase transformation, densification and crystallization behavior of α-cordierite phase. Sintering and crystallization behavior was observed by dilatometry test, non-isothermal DTA, and XRD, respectively. The existence of Fe_2O_3 in the minerals has resulted in greenish glass frits, while CaO, K and other impurities act as modifying oxide in glass compositions, reducing the viscosity of the glass, and thus affect phase transformation of glass. Although the dielectric loss of the sample from mineral precursors was slightly higher than the sample from reagent grade oxides, other properties gained were comparable and not varies too much.

1. Introduction

The replacement of raw materials from reagent grade oxides to natural resources for product processing has been extensively studied over the years. Besides searching for better material characteristics and properties by modification of chemical substitutes and processing parameters and methods, researchers in material science have focused on discovering cheaper substitutes for common raw materials. α-Cordierite is a crystalline ceramic that can be synthesized using various methods and raw materials. The difficulty of obtaining dense α-cordierite glass-ceramic with high purity and crystallinity at low sintering temperatures (≤900 °C) has been reported in the literature [1–4]. Recently, we have successfully produced high purity and dense α-cordierite phase at a low temperature using mainly talc and kaolin as initial raw materials through stoichiometric modification using minerals, crystallization of glass method, and mechanical activation with high energy mill [5]. In the present study, the above composition was reproduced using the same raw materials (mainly talc and kaolin) while another composition was produced using high purity oxides (MgO, Al_2O_3, and SiO_2). Although many studies on non-stoichiometric cordierite using reagent grade oxides as starting raw materials [1,2,6–11] have been conducted, the processing parameters used were different and none of them used the exact same mole ratio as above. Even if the same compositions were used, the slightest difference in processing steps and processing parameters will significantly change the final properties of the bulk samples. For instance, the melting temperature and quenching rate will determine whether the compound fully transforms into the amorphous phase or not. The selections of melting temperature will affect the viscosity of molten glass. The higher the melting temperature, the higher the viscosity of the glass will be. Therefore, if the same quenching parameter is used, different volume and different density of the glass would be obtained. The silicate chain might be arranged in close or open manner, and the bond length might varies depends on the viscosity of glass before quenching. As a result, the quenched glass with different degree of silicate chain arrangement would attain different interfacial energy, thus cause variation in nucleation rate.

Moreover, variation in the melting process may also result in devitrification of the glass and consequently, the existence of small amounts of the polycrystalline phase in the matrix of amorphous glass powder will change the mechanism of sintering. At the same time, selection of grinding media and grinding parameters in the frit pulverization process yields different particle sizes, shapes, distribution, and also types of impurities in the samples. This will consequently vary the type and phase content in the samples. Therefore, it is important to fix and control the processing parameters in order to make a comparison between the two different starting raw materials as well as to determine the effects of the existence of impurities in the minerals to the properties of obtained glass ceramic.

* Corresponding author. Tel.: +60 4 5996128; fax: +60 5 5941011.
E-mail address: zainal@eng.usm.my (Z.A. Ahmad).

0925-8388/$ – see front matter © 2011 Elsevier B.V. All rights reserved.
doi:10.1016/j.jallcom.2011.04.129

Table 1
Elemental analysis minerals and reagent grade oxides compound by XRF.

	Kaolin (wt%)	Talc (wt%)	SiO_2 (wt%)	Al_2O_3 (wt%)	MgO (wt%)
MgO	0.88	49	–	–	99
SiO_2	59	47	99.5	0.2	–
Al_2O_3	35	0.16	0.04	99.46	–
K_2O	3	–	–	–	–
CaO	0.014	3	–	0.075	0.13
TiO_2	0.84	–	–	–	–
Fe_2O_3	0.6	0.45	0.04	0.15	0.0036
Cr_2O_3	0.032	–	–	–	–
NiO	0.014	0.028	–	0.022	–
P_2O_5	0.073	0.095	–	–	–
ZrO_2	0.05	–	–	–	–
SO_3	–	0.055	–	–	0.07
CuO	–	0.016	–	0.014	–

Talc and kaolin normally contain small amounts of impurities which are from alkali metal oxide and alkaline earth oxide groups. These impurities will play a role as modifying oxides in the glass structure by weakening the bonds within the glass network [12]. It may accommodate the holes or interstices in the random network structure or between tetrahedral groups and will result in changes of the properties, including reduction of viscosity of the glass. Aluminum oxide, which is one of the main constitutions in this glass composition, will form a tetrahedral group and therefore, is able to replace SiO_4 tetrahedral in the silicate lattice. Since the aluminum ion has a charge of 3^+ as compared to the silicon ion with a charge of 4^+, additional positive charge must be present to ensure electroneutrality. The existence of one alkali metal ion (originating from the minerals) per AlO_4 tetrahedron would satisfy this requirement, thus will significantly influence the crystallization of glass. Thus, in the present study, non-stoichiometric cordierite compositions from both groups of raw materials were synthesized using the same steps and parameters in order to make a comparison of their densification, crystallization and properties. The results were analysed to certify the worth of replacing the reagent grade oxides commonly being used today with minerals.

2. Materials and methods

α-Cordierite with the chemical formulation $2.8MgO{\cdot}1.5Al_2O_3{:}5SiO_2$ was synthesized using two different types of initial raw materials. One group was synthesized from mainly talc and kaolin with a small addition of reagent grade oxides to compensate the required MAS ratio, while the other group was synthesized using reagent grade oxides (MgO, Al_2O_3, and SiO_2). The kaolin was obtained from Kaolin Industry, Tapah Perak, Malaysia, talc and silica from Ipoh Ceramic Sdn. Bhd., alumina from Metco and magnesia from Merck. An elemental analysis of the raw materials is given in Table 1, while Table 2 gives details on weight percent of initial raw materials. The amount of talc and kaolin used in each compositions studied was weighted to the optimum amounts in order to minimize the use of pure metal oxides. Excess total weight % in mineral precursor samples is due to the total impurities in the minerals. The homogeneous mixture of compounds was melted at 1500 °C in alumina crucibles. After 4 h of soaking at the respective temperatures, the samples were immediately quenched in distilled water to form frits, followed by drying to remove moisture. All frits were milled using the same milling parameters to obtain glass powders with average particle sizes in the range of 1–3 μm.

XRD of the glass powder and sintered pellet was carried out to determine the evolution of the glassy phase to the crystalline state. The XRD patterns of the glass and sintered products were obtained using a Bruker D8 Advanced operated in Bragg–Brentano geometry, with Cu Kα radiation, in the $10^\circ \leq 2\theta \leq$ to 90° range. Counting time was fixed at 71.5 s for each $0.03^\circ 2\theta$ step. The X-ray tube was operated at 40 kV. Quantitative analysis was revealed by Rietveld method using HighScore Plus software. DTA analyses were carried out using DTA machine Model Linseis. Experimental was conducted using non-isothermal profile heating at 5 K/min from 38 °C to 1000 °C. Green body samples were prepared by compacting the glass powder using a Hydrotex uniaxial pressing machine at 120 MPa and sintering at 900 °C for 2 h with 5 K/min heating rate prior to XRD, density, CTE, and dielectric test. Shrinkage analysis of green samples was carried out using a high temperature vertical dilatometer (Linseis) from room temperature to 1100 °C. The microstructure of the fractured and etched samples was observed using field emission scanning electron microscopy (VP FESEM-Supra 35VP) at 30 kV. CTE test was carried out on the sintered samples using high temperature vertical dilatometer tests (Model Linseis) in air from room temperature to 1000 °C, while the dielectric measurements were made using an Impedance Analyzer (Hewlet Packard model HP4291). The density and porosity were measured using the Archimedes principle.

Table 2
Composition (wt%) of initial raw materials for both samples (pure oxides and minerals) with formulation $2.8MgO{\cdot}1.5Al_2O_3{\cdot}5SiO_2$.

Sample	Reagent grade oxides (sample P)	Minerals (sample A)
Talc (wt%)	–	31
Kaolinite (wt%)	–	65
MgO (wt%)	19.93	4.74
Al_2O_3 (wt%)	27.01	4.26
SiO_2 (wt%)	53.06	0.14
Total (wt%)	100	105.14

3. Results and discussion

3.1. Characterization of glass frits and glass powder

A frit from reagent grade oxides is white in color, while a frit from minerals is of a greenish color. The presence of about 1 wt% iron oxide, Fe_2O_3, in the minerals confers the greenish color to the glass, as shown in Fig. 1. Both frits are transparent which indicate that they are in glassy forms. The molecules in the glass are not stacked neatly. Random organization of glass causes the formation of gaps and holes which allow portions of light waves to pass through. The greater the randomness of the molecules in the substances, the easier the light can pass through. The glass reflects very little light because its index of reflection is fairly closed to the air. Therefore, photons that are not reflected will interact with the atoms of molecules and are reemitted, giving a transparent look. The electrons in the glass absorb the energy of photons in the UV range. Therefore, if the electron absorbs the energy of any portion of the visible spectrum, the light that transmits through will appear colored accordingly to that portion of the spectrum. Thus, the color of the frits is a result of the energy levels of the electrons in the substance.

X-ray diffraction of fine glass powders (Fig. 2) shows only diffuse halos. Therefore, these compositions are suitable to be melted using the particular melting parameter.

3.2. Non-isothermal differential thermal analysis

Crystallization of the amorphous phase was studied by DTA in non-isothermal profile heating. DTA plots for both samples are demonstrated in Fig. 3. Sample synthesized from minerals has a slightly lower crystallization temperature (measured at maximum peak) than samples synthesized from reagent grade oxides. The existence of impurities in the samples may cause local fluctuations in the structure, thus giving rise to the nucleation process. Low viscosity of the glass contributed from extra modifying oxides in the samples synthesized from minerals will also enhance the diffusion rate. However, based on the area under the DTA peak, sample synthesized from reagent grade oxides have a higher degree of crystallinity compared to samples synthesized from mainly talc and kaolin. This result was supported by X-ray diffraction pattern of the sintered pellets (Fig. 4), whereby with the same composition, samples obtained from reagent grade oxides have higher counts of intensity.

3.3. Phase analysis by X-ray diffraction

Fig. 4 shows the X-ray diffraction pattern of sintered pellets which were heat treated at 900 °C for 2 h. It can be obviously seen that samples A and P were fully crystalline when heated

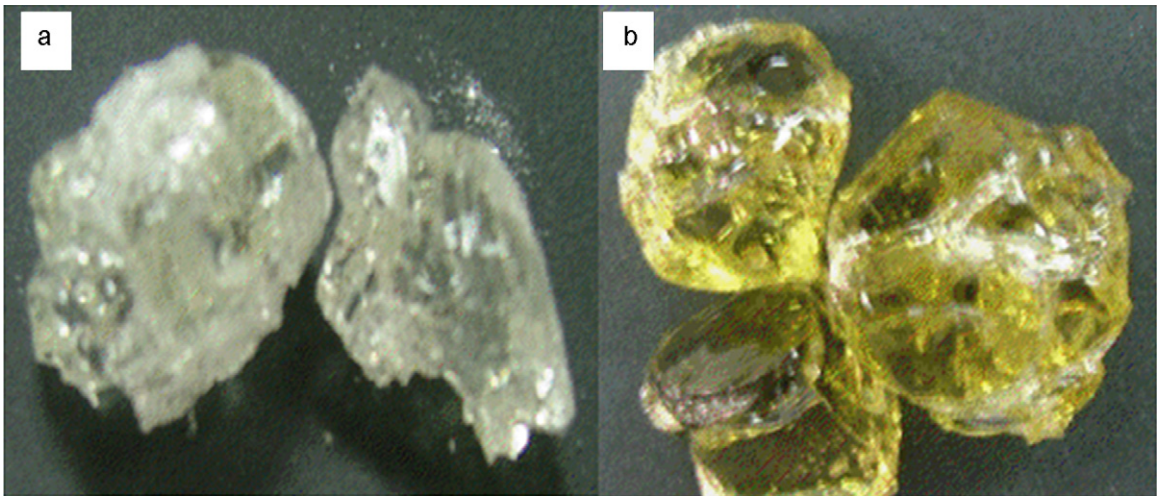

Fig. 1. Photograph of frits for non-stoichiometric samples with different initial raw materials; (a) reagent grade oxides and (b) minerals.

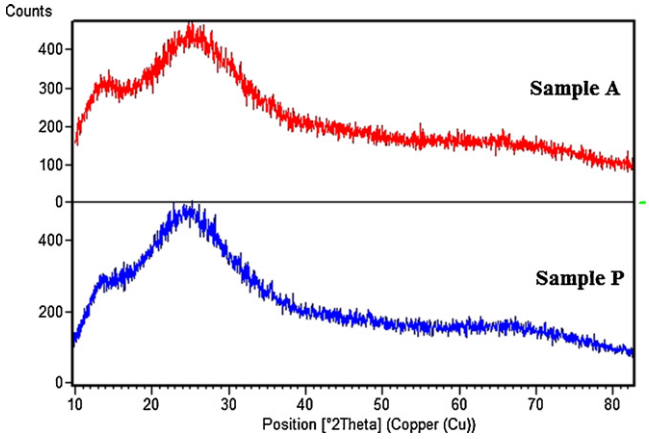

Fig. 2. X-ray diffraction pattern of glass powder.

at this sintering parameter. Excess MgO and less Al_2O_3 from the stoichiometric composition contributed in enhancing the crystallization behavior of α-cordierite. μ-Cordierite phase still existed as a secondary phase in sample P. However, peaks that belong to μ-cordierite were not observed in sample A. Sample A reveals single phase α-cordierite. Close observations of the diffraction pattern of the sintered pellet demonstrate the variation of intensity ratio of the α-cordierite peak between samples A and P. The ratio of intensity between the strongest peak of α-cordierite (which was located at 2θ 10.25°) to other α-cordierite peaks in the same diffraction pattern was obviously higher in the diffraction pattern of sample P compared to sample A. We have confirmed that the difference in the α-cordierite relative intensity between the two samples was neither due to the preferred orientation derived from the sample preparation procedure nor instrumental error since repetition on sample preparation during X-ray diffraction measurement was done on the above sample. However, other planes show similar counts, as can be seen from the zoom in Fig. 5.

3.4. Rietveld quantitative phase analysis

Quantitative phase analysis of heat treated glass samples demonstrated that the compacted glass of sample A had crystallized to 100 wt% α-cordierite phase. On the other hand, the glass of sample P had crystallized to α-cordierite and μ-cordierite phase. Verification of single-phase α-cordierite formation was confirmed by Rietveld structure refinement using HighScore Plus software with better fitting between the measure and calculated pattern. Table 3 shows quantitative phase analysis of heat treated samples synthesised from reagent grade oxides and minerals of the same MAS ratio. It shows that besides α-cordierite, sample P also contains 6.1 wt% μ-cordierite phase. Results of analysis on both samples give low agreement indices, *R*-factors, which reflect how good the fit is

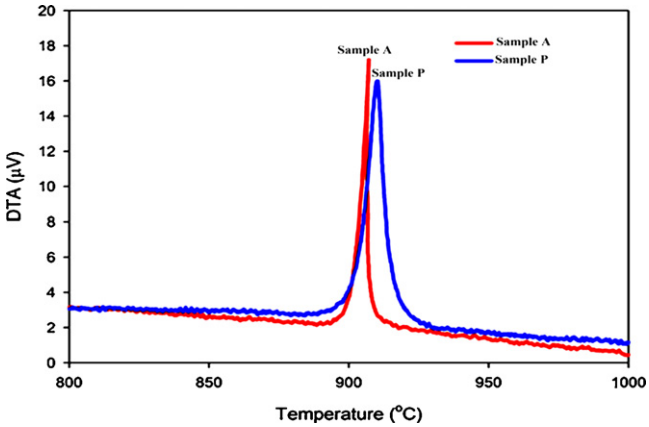

Fig. 3. Non-isothermal DTA analysis of samples with different initial raw materials; (a) minerals and (b) reagent grade oxides.

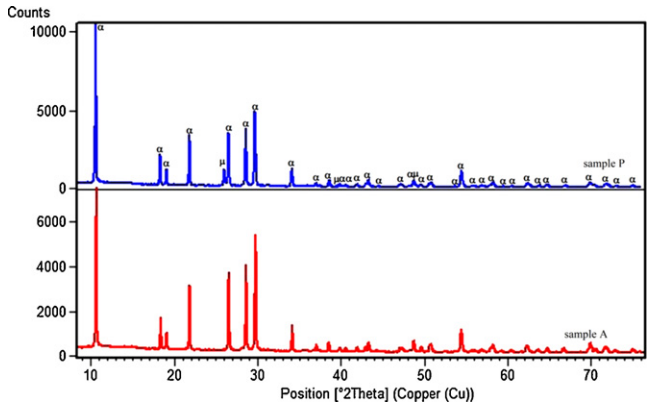

Fig. 4. X-ray diffraction pattern of heat treated compacted glass powder samples synthesized from reagent grade oxides (sample P) and minerals (sample A).

Table 3
Quantitative phase analysis of heat treated sample synthesis from reagent grade oxides and minerals of the same MAS ratio.

Sample	Phases	Quantity (wt%)	Crystal density	R_{bragg}	R_{wp}	GOF	R_{exp}	R_p
Sample A	α-Cordierite	100	2.54	11.52	9.55	1.55	6.17	7.5 0
Sample P	α-Cordierite	87.8	2.52	4.74	8.26	1.583	6.56	5.83
	μ-Cordierite	6.1	2.58	5.98				

to the entire pattern. The high R_{bragg} in sample A as compared to sample P was caused by bad quality fitting in α-cordierite peak at the 0 1 0 plane.

3.5. Lattice parameter

Table 4 gives crystal structure data of α-cordierite synthesized from different raw materials. The lattice parameter as well as the volume of α-cordierite crystal of sample A is slightly higher than sample P. The expansion of lattice may have resulted from interstitial impurities atoms which originated from the minerals e.g. K_2O, CaO, TiO_2 and Fe_2O_3. Due to this sample A also possessed higher crystallite size (208.6 nm) as compared to sample P (152 nm)

3.6. Dilatometry

The sintering reaction of each sample during heating from 38 °C to 1000 °C was observed by dilatometry test of compacted green samples. It can be seen from Fig. 6 that both samples synthesized from mainly talc and kaolin started to shrink at a low temperature, approximately at 775 °C, while sample synthesized using reagent grade oxides began at 825 °C. Most of the samples shrunk at the same amount i.e. around 12%. However, the sample from minerals stopped densifying at a much lower temperature.

The existence of alkali oxide (K_2O) and alkaline earth oxides (CaO) are contributed to lowering softening characteristics of sample A. Small amounts of K_2O and CaO could play a role as modifying oxides when it was introduced into silicate glasses. The metallic cations occupying the holes or interstitial positions and the oxygen ions contributed to the glass becoming links to the network, forming ions (e.g. silicon) in the random network structure. Instead of the bridging oxygen ions which formed the link between two SiO_4 tetrahedral, the existence of these oxides will weaken the glass network thus causing non-bridging oxygen. This in turn results in changes of the properties including reduction of the viscosity of the glass [12]. The viscosity of glass can be evaluated either by measuring the rate of neck formation between two glass beads, or measuring the rate of densification of glass powder compacts, or measuring the glass transition temperature.

Therefore, based on the observation in dilatometry curve, the existence of alkali and alkaline earth oxides in sample A cause it to possesses lower softening temperature than sample P. This indicates that sample P has to overcome much higher energy barrier before it can flow as compared to sample A. The existence of mixed alkali oxide in sample A had accelerated the densification of glass and this has resulted in earlier completion of densification as shown in Fig. 6. Rapid densification started when the glass attained sufficient fluidity to consolidate the glass particles by capillary forces. Therefore, easier densification in sample A as compared to sample P might results from the variation of viscosity in the samples. Since the viscosity decreases when the sintering temperature increases, a higher sintering temperature results in easier densification. As a result, sample A completely densified at 825 °C, while sample P at 925 °C.

3.7. Activation energy for densification

A comparison of activation energy for densification between reagent grade oxides and minerals samples are tabulated in Table 5. Glass samples synthesized from reagent grade oxides have higher activation energy for densification than samples synthesized from minerals. The existence of alkaline earth oxide and alkali metal oxide in the minerals decreased the viscosity of the glass, thus making densification easier at lower temperatures than samples synthesized from reagent grade oxides.

3.8. Densification and crystallization behavior

Densification and crystallization temperatures of both reagent grade oxides and minerals samples are presented in Fig. 7. As shown in the graph, crystallization occurs after densification has stopped for both of samples. Glass sample synthesized from minerals have

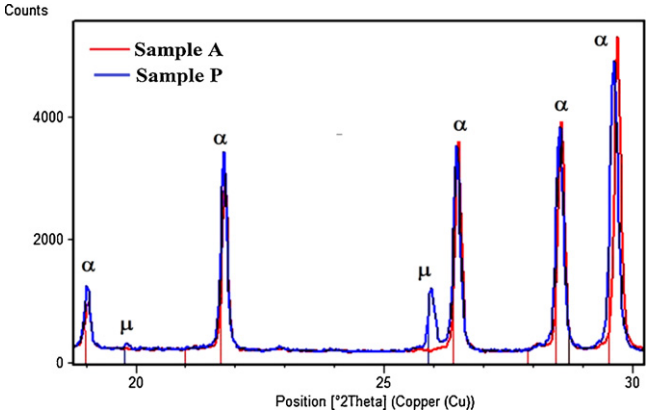

Fig. 5. Diffraction curves of green rectangular pellets for both sintered samples zoom in 2 theta 18.8–30°. (For interpretation of references to color in this figure legend, the reader is referred to the web version of this article.)

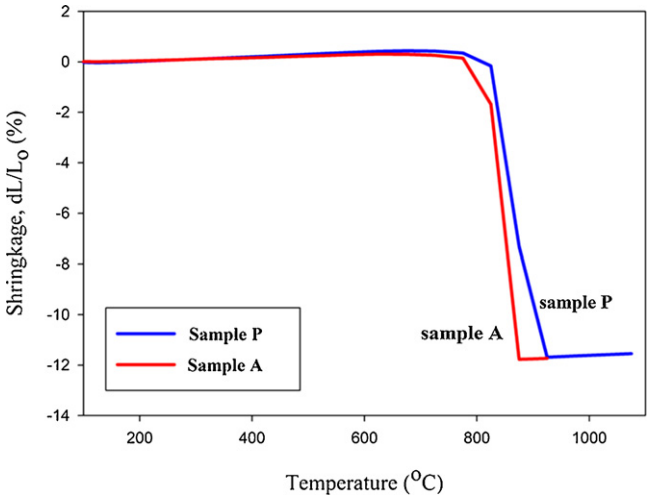

Fig. 6. Dilatometry curve of green rectangular pellets for both samples heating at increment temperature. (For interpretation of references to color in this figure legend, the reader is referred to the web version of this article.)

Table 4
Comparison on crystal structure of α-cordierite phase in sample synthesized from reagent grade oxides and minerals.

	Lattice *a* (Å)	Lattice *c* (Å)	Crystal volume (Å^3)	Crystal density (g/cm^3)	Crystallite size (nm)
Sample A	9.79934 (0.005)	9.38761 (0.005)	772.74	2.51 (0.01)	208.6 (13)
Sample P	9.74375 (0.005)	9.34806 (0.005)	768.1	2.53 (0.01)	152.5 (20)

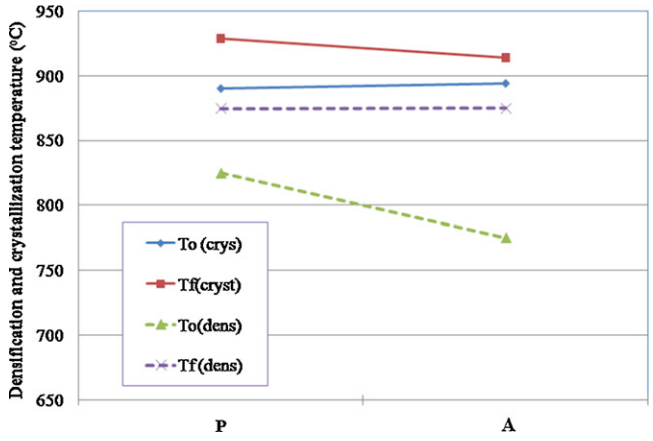

Fig. 7. Densification and crystallization temperature of glass powder samples synthesized from reagent grade oxides and minerals.

Table 5
Activation energy for densification for reagent grade oxides and minerals glass samples with composition 2.8MgO·1.5Al$_2$O$_3$·5SiO$_2$.

	Activation energy for densification (KJ/mol)
Sample A	364 (5)
Sample P	732 (8)

lower densification and crystallization temperatures than sample synthesized from reagent grade oxides.

3.9. Density, porosity and shrinkage

Table 6 indicates results of density, percentage of porosity and shrinkage for both samples sintered for 2 h at 900 °C. Both samples were fully densified with similar density, percentage of shrinkage and porosity.

3.10. Microstructure analysis

The dilatometry curve reveals that the glass powder required a temperature of about 825 °C for sample A and 925 °C for sample P, respectively, to obtain constant shrinkage of the compacted pellet if it was heated in non-isothermal conditions. However, the microstructure of samples coupled with results of porosity and density proved that sample P also fully densified at 900 °C when soaked for 2 h. The shrinkage, $\Delta L/L_0$, of a compact composed of spherical particles of radius, *r*, takes place through flow driven by surface tension, γ, can be given in the following expression [13]:

$$\frac{\Delta L}{L_0} = \frac{3\gamma}{8\gamma\eta(T)t}$$

where L_0 is initial length of the compact, and *t* is time. Therefore, the shrinkage as well as diffusion process is time dependent. Viscous sintering occurs by material flows driven by capillarity, Thus, prolong soaking for 2 h enhanced the diffusion process, thus even at temperature below 925 °C, sample P could densify as good as sample A. Figs. 8 and 9 show the microstructure of etched (etched with 5 M HF) and fracture sintered samples. FESEM microstructure analysis reveals that sample A has better densification than sample P and the apparent porosity level of sample P is higher than sample A. The existence of small amounts of alkaline earth in the initial raw materials reduced the melting temperature and viscosity of the glass. Thus, during crystallization heat treatment process, the viscous flow is more effective in eliminating the pores

3.11. Dielectric properties

Fig. 10 shows results of dielectric constant of samples as a function of frequency. It was clearly demonstrated that sample synthesized from reagent grade oxides have lower dielectric constant compared to sample synthesized from mainly talc and kaolin. Sample A has a slightly higher dielectric constant than sample P due to its better densification behavior. However, the dielectric constants of both samples are within the standard value.

Fig. 11 reveals the dielectric loss of samples as a function of frequency. It shows that sample A has higher dielectric loss compared to sample P. Microstructure analysis of etched surface indicates that sample A has larger grain size compared to other samples. As discussed above, densification and crystallization started and finished at lower temperatures and earlier times in sample A than sample P. Therefore, under the same profile heat treatment, this caused the tendency of grain to growth in sample A and finally resulted in large grain size with low porosity.

3.12. Coefficient of thermal expansion

Dilatometry test was also performed on sintered rectangular samples to determine the linear thermal expansion of α-cordierite as a function of temperature. The CTE for both sintered mineral and pure oxides samples is shown in Table 7. Sample P synthesized from pure oxides has lower CTE than sample A (synthesized from minerals). As the CTE of materials is greatly dependent on the bond strength between the atoms, the existence of mixed alkali oxides in sample A will acted as a modifying oxides and

Table 6
Bulk density, percent of porosity and shrinkage of sintered sample.

	Density (g/cm^3)	Shrinkage (%)	Porosity (%)
Sample A	2.54 (0.02)	12.44 (0.05)	0.44 (0.01)
Sample P	2.54 (0.02)	12.59 (0.07)	0.58 (0.02)

Table 7
Coefficient of thermal expansion of sintered pellet.

Sample	CTE (°C^{-1})
Sample A	2×10^{-6}
Sample P	3×10^{-7}

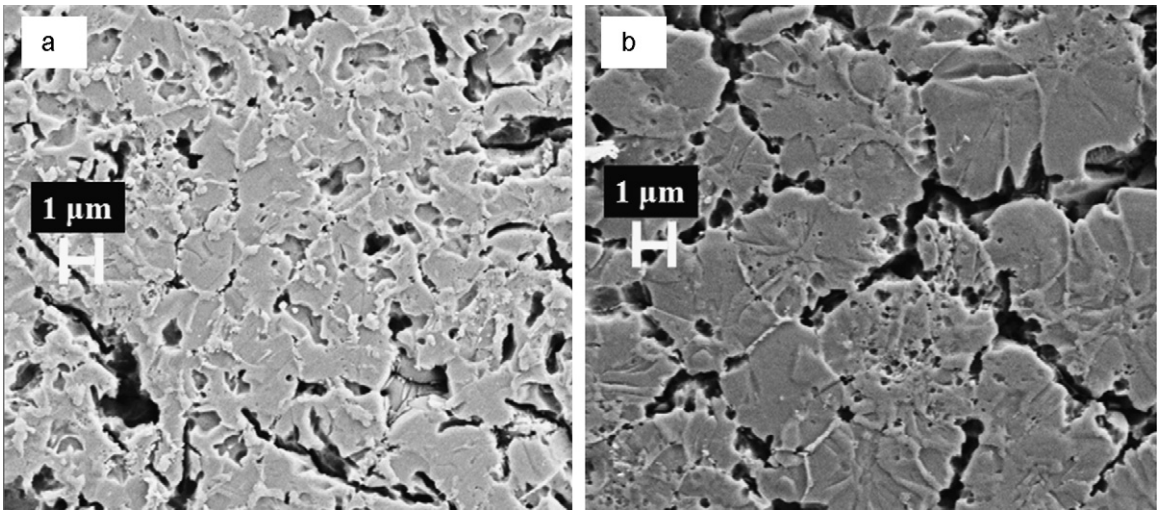

Fig. 8. Microstructure of sintered and etched surface for sample synthesized from reagent grade oxides and minerals.

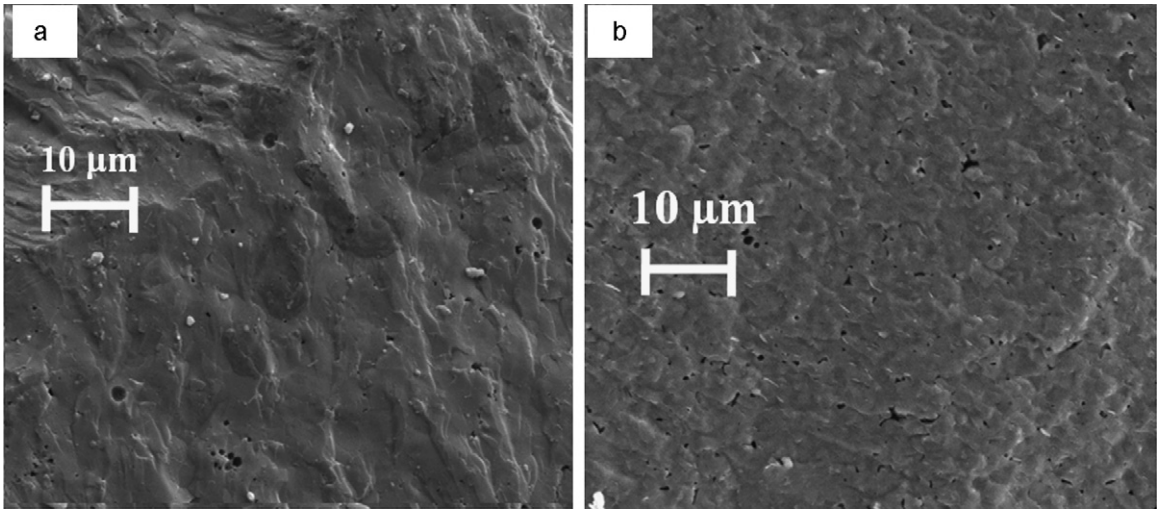

Fig. 9. Microstructure of fractured surface of sintered pellets synthesized from reagent grade oxides and minerals.

might distorted some of the silicate chains, thus, decrease the rigidity of the network structure [14]. The mixed alkali oxides were expected to be interstitial inside the two structure holes or interstitial vacant sites that were present per unit formula in the *c*-axis of α-cordierite structure [15]. Lower CTE in sample P may have also resulted from the existence of higher micro pores due to the existence of other secondary phase as compared to sample A.

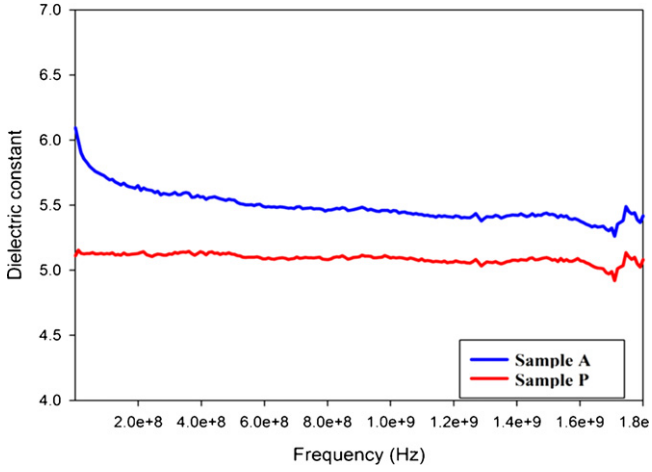

Fig. 10. Dielectric constant of both samples synthesized from reagent grade oxides and minerals as a function of frequency.

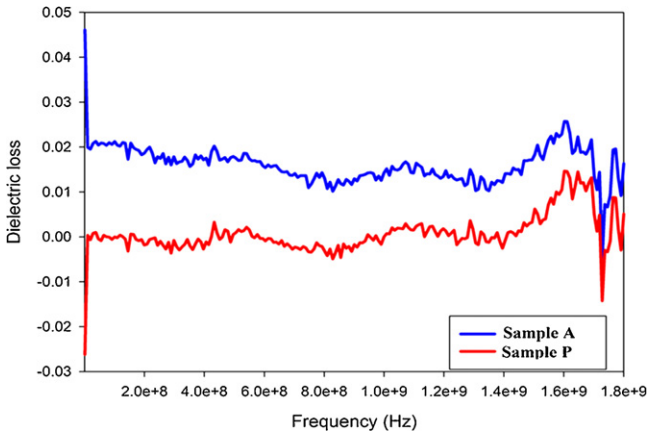

Fig. 11. Dielectric loss of heat treated glass samples synthesized from reagent grade oxides and minerals as a function of frequency samples as a function of frequency.

4. Conclusions

A high degree of α-cordierite phase was crystallized and produced using both samples from reagent grade oxides and minerals. Dense structures were obtained even without sintering aids. The sample synthesized from mainly talc and kaolin had better densification and crystallization behaviors, compared to the sample synthesized from reagent grade oxides. The existence of impurities (Fe_2O_3) in the composition caused the frits to appear a transparent greenish color, and other impurities (CaO, K_2O) could react as a modifying oxide to enhance the densification and crystallization of α-cordierite. Activation energy for the densification of samples synthesized from minerals had much lower values than the samples from reagent grade oxides. The disadvantage is only in the dielectric loss, where the non-stoichiometric samples synthesized from mainly talc and kaolin had slightly higher dielectric loss, but is still in a low range for application as a substrate in high frequency applications.

Acknowledgements

The authors gratefully acknowledge the financial support from the Islamic Development Bank Scholarship Programme and Fundamental Research Grant Scheme (9003-00171) Universiti Malaysia Perlis, and technical assistants from Universiti Sains Malaysia (USM).

References

[1] D.T. Weaver, D.C.V. Aken, J.D. Smith, J. Mater. Sci. 39 (2004) 51–59.
[2] A. Goel, E.R. Shaaban, F.C.L. Melo, M.J. Ribeiro, J.M.F. Ferreira, J. Non-Cryst. Solids 353 (2007) 2383–2391.
[3] V.K. Marghussian, U. Balazadegan, B. Eftekhari-yekta, J. Eur. Ceram. Soc. 29 (2009) 39–46.
[4] F.J. Torres, J. Alarcon, J. Eur. Ceram. Soc. 23 (2003) 817–826.
[5] J. Banjuraizah, H. Mohamad, Z.A. Ahmad, J. Alloys Compd. 482 (2009) 429–436.
[6] A.H.H. Rachman Chaim, J. Am. Ceram. Soc. 75 (1992) 1512–1521.
[7] G.-H. Chen, X.-Y. Liu, J. Alloys Compd. 431 (2007) 282–286.
[8] G.-h. Chen, J. Alloys Compd. 455 (2008) 298–302.
[9] S. Wang, H. Zhou, L. Luo, Mater. Res. Bull. 38 (2003) 1367–1374.
[10] T. Rudolph, W. Pannhorst, G. Petzow, J. Non-Cryst. Solids 144 (1993) 273–281.
[11] S.-H. Lo, C.-F. Yang, Ceram. Int. 24 (1998) 139–144.
[12] P.W. McMillan, Glass-Ceramics, Academic Press Inc., London, 1969.
[13] M.O. Prado, M.L.F. Nascimento, E.D. Zanotto, J. Non-Cryst. Solids 354 (2008) 4589–4597.
[14] P. Pisciella, M. Pelino, J. Eur. Ceram. Soc. 28 (2008) 3021–3026.
[15] B.P. Saha, R. Johnson, I. Ganesh, G.V.N. Rao, S. Bhattacharjee, Y.R. Mahajan, Mater. Chem. Phys. 67 (2001) 140–145.